JOC Article

Correlated Rotations in Benzylfluorene Derivatives: Structure, Conformation, and Stereodynamics

Daniele Casarini,*,† Lodovico Lunazzi,‡ and Andrea Mazzanti*,‡

Department of Chemistry, University of Basilicata, via N. Sauro 85, Potenza 85100, Italy and Department of Organic Chemistry "A. Mangini", University of Bologna, Viale Risorgimento 4, Bologna 40136, Italy

casarini@unibas.it; mazzand@ms.fci.unibo.it

Received December 18, 2007

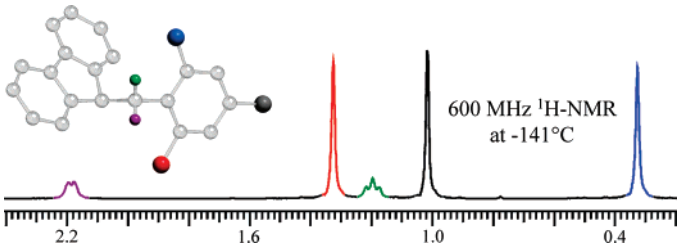

Fluorene derivatives, having substituted benzyl groups bonded to position 9, have been investigated by variable temperature NMR spectroscopy. Stereodynamic processes involving restricted rotation about the fluorenyl−CH_2 and aryl−CH_2 bonds have been observed, leading to conformers and enantiomeric forms, and the corresponding barriers were determined by line shape simulation. These dynamic processes are interpreted as being due to correlated rotation pathways, on the basis of DFT computations that satisfactorily reproduce the experimental barriers. The structures of two such compounds were also determined by single-crystal X-ray diffraction

Introduction

The study of fluorenyl derivatives has received considerable attention owing to the circumstance that the fluorene motif appears in a number of molecules with possible applications in material science.[1−4] The 9-arylfluorenyl derivatives also display dynamic processes that have been investigated by variable temperature NMR spectroscopy.[5] All the compounds investigated so far have an aryl group directly bonded to position 9 of the fluorenyl moiety so that only one kind of bond rotation process could be detected. Here we present a number of fluorene derivatives bearing susbstituted benzyl moieties at position 9, thus making possible the detection of two concomitant rotation processes, as well as the identification of stereolabile isomers (conformers) of different stabilities. For this purpose we synthesized the compounds displayed in Chart 1, where the isopropyl group was introduced for monitoring the possible asymmetry of the conformers.

Results and Discussion

As shown in the NMR spectrum of Figure 1, the ^{1}H doublet signal for the isopropyl methyl groups of compound **1** broadens below −120 °C and eventually splits into two signals of different intensities (94:6) at −157 °C. Analogous splitting was also observed for all the other three aliphatic signals. The major interconverts into the minor conformer with a free energy of activation of 6.0 kcal mol^{-1} (Table 1), this value deriving from the rate constants used for the simulation of the spectrum of Figure 1. Both the methyl signals of the major and of the minor conformer appear as single signals at −157 °C, indicating that the pairs of methyls on an isopropyl group are not diastereotopic

† University of Basilicata.
‡ University of Bologna.

(1) Grell, M.; Knoll, W.; Lupo, D.; Meisel, A.; Miteva, T.; Neher, D.; Noyhofer, H.-G.; Scherf, U.; Uasuda, A. *Adv. Mater.* **1999**, *11*, 671−675.
(2) Rathore, R.; Abdelwahed, S. H.; Guzei, I. A. *J. Am. Chem. Soc.* **2003**, *125*, 8712−8713.
(3) Geng, Y.; Trajkovska, A.; Culligan, S. W.; Ou, J. J.; Chen, H. M. P.; Katsis, D.; Chen, S. H. *J. Am. Chem. Soc.* **2003**, *125*, 14032−14038.
(4) Nakano, T.; Yade, T. *J. Am. Chem. Soc.* **2003**, *125*, 15474−15484.
(5) Siddall, T. H., III; Stewart, W. E. *Chem. Commun.* **1968**, 1116. Siddall, T. H., III; Stewart, W. E. *Tetrahedron Lett.* **1968**, *9*, 5011. Chandross, E. A.; Sheley, C. F., Jr. *J. Am. Chem. Soc.* **1968**, *90*, 4345. Rieker, A.; Kessler, H. *Tetrahedron Lett.* **1969**, *10*, 1227. Bartle, K. D.; Bavin, P. M .G.; Jones, D. W.; L'Amie, D. *Tetrahedron* **1970**, *26*, 911. Nakamura, M.; Oki, M. *Tetrahedron Lett.* **1974**, *15*, 505. Ford, W. T.; Thompson, T. B.; Snoble, K. A.; Timko, J. M. *J. Am. Chem. Soc.* **1975**, *97*, 95. Albert, K.; Rieker, A. *Chem. Ber.* **1977**, *110*, 1804. Nakamura, M.; Nakamura, N. Oki, M. *Bull. Chem. Soc. Jpn.* **1977**, *50*, 2986. Murata, S.; Kanno, S.; Tanabe, Y.; Nakamura, M.; Oki, M. *Bull. Chem. Soc. Jpn.* **1982**, *55*, 1522. Tukada, H.; Iwamura, M.; Sugawara, T.; Iwamura, H. *Org. Magn. Res.* **1982**, *19*, 78. Lam, Y.-L.; Koh, L.-L. Huang, H.-H.; Wang, L. *J. Chem. Soc., Perkin Trans. 2* **1999**, 1137.

10.1021/jo7026917 CCC: $40.75
Published on Web 03/08/2008

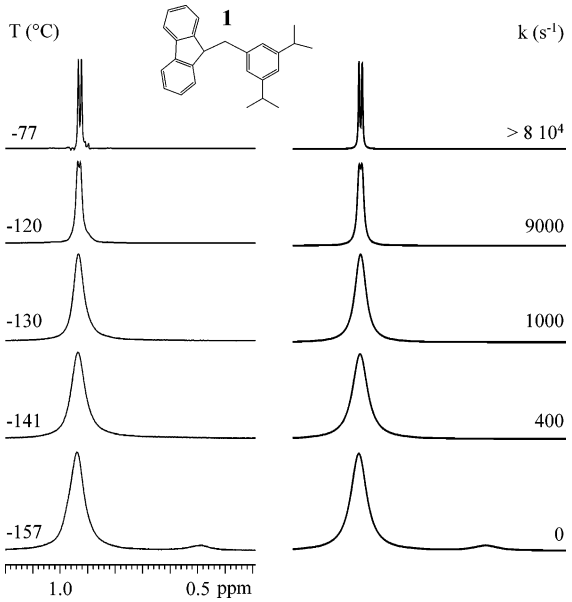

FIGURE 1. Temperature dependence of the methyl signal (600 MHz in $CHF_2Cl/CHFCl_2$) of compound **1** (left). On the right the spectral simulation with the rate constants indicated.

TABLE 1. Experimental and DFT Computed Barriers (kcal mol^{-1}) of Compounds 1−5

compd	type of motion (see text)	experimental	computed
1	conformer interconversion	6.0[a]	5.5
2	enantiomerization	7.4	7.0
3	homomerisation	11.7	11.7
	enantiomerization	7.9	7.4
4	conformer interconversion	5.3[a]	4.7
5	conformer interconversion	5.6[a]	4.65

[a] The barriers refer to the interconversion of the major into the minor conformer.

CHART 1

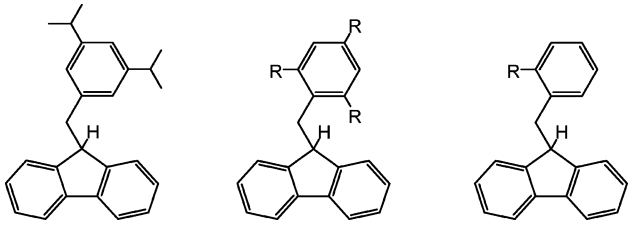

1 R=Me, **2** R=Pr^i, **3** R=Me, **4** R=Pr^i, **5**

(the viscosity broadened spectrum at such low temperatures does not allow one to observe the splitting due to the *J* coupling with the isopropyl methine hydrogen). Due to the frozen rotation about the fluorene−CH_2 bond, the existence of two conformers with different populations could be observed in the spectrum at −157 °C: on the contrary, the rotation about the Ar−CH_2 bond (Ar being the di-isopropylphenyl moiety) is still fast at that temperature, thus explaining why the expected diastereotopicity of the isopropyl methyl groups was not detected.

DFT computations[6] predict that in compound **1** the two lowest energy minima, separated by 1.2 kcal mol^{-1}, correspond to the two conformers (labeled A and B) shown in Scheme 1. Conformer A, where the aryl and the fluorenyl moieties are in an *anti* relationship, has an energy lower than that of B, where these moieties are in a *syn* relationship. Conformer A might

SCHEME 1. Schematic Representations and Corresponding Newman Projections of the Two Most Stable Conformers of Compound 1[a]

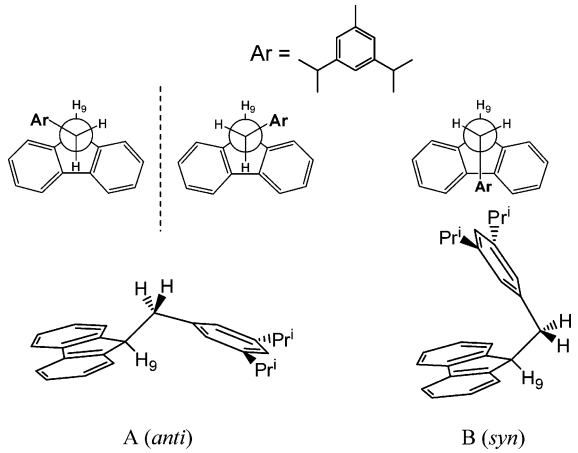

[a] See also Figure S-1 of the Supporting Information.

exist as a pair of conformational enantiomers (displayed in the corresponding Newman projections on the top left of Scheme 1) that interconvert, however, with a barrier too low for NMR detection (computed value 3.6 kcal mol^{-1}). The corresponding transition state has a C_s symmetry, thus the conformer A (*anti*), involved in such a rapid interconversion, is perceived by NMR as having, in practice, a dynamic C_s symmetry and, as such, is schematized in Scheme 1. The same calculations[6] also predict that the rotation barrier about the fluorenyl−CH_2 bond, required to accomplish the A to B interconversion, is 5.5 kcal mol^{-1}, a value in agreement with the measured barrier (6.0 kcal mol^{-1}) for the observed exchange of the two conformers. These theoretical results thus explain the spectral appearance of compound **1** as a function of temperature.

Contrary to the case of **1**, the low-temperature NMR spectrum of **2** indicates that only a single conformer is populated:[7] this conformer undergoes a dynamic process, because anisochronous signals are observed at low temperature for the *ortho* methyl groups and for the methylene hydrogens (Figure 2). The spectral simulation was obtained by using a single rate constant, and the barrier derived from the reported *k* values is 7.4 kcal mol^{-1} (Table 1): the same barrier was also obtained by monitoring the ^{13}C signal of the *ortho* quaternary carbons of the mesityl moiety (Figure S-2 of the Supporting Information).

(6) Frisch, M. J.; Trucks, G. W.; Schlegel, H. B.; Scuseria, G. E.; Robb, M. A.; Cheeseman, J. R.; Montgomery, J. A., Jr.; Vreven, T.; Kudin, K. N.; Burant, J. C.; Millam, J. M.; Iyengar, S. S.; Tomasi, J.; Barone, V.; Mennucci, B.; Cossi, M.; Scalmani, G.; Rega, N.; Petersson, G. A.; Nakatsuji, H.; Hada, M.; Ehara, M.; Toyota, K.; Fukuda, R.; Hasegawa, J.; Ishida, M.; Nakajima, T.; Honda, Y.; Kitao, O.; Nakai, H.; Klene, M.; Li, X.; Knox, J. E.; Hratchian, H. P.; Cross, J. B.; Bakken, V.; Adamo, C.; Jaramillo, J.; Gomperts, R.; Stratmann, R. E.; Yazyev, O.; Austin, A. J.; Cammi, R.; Pomelli, C.; Ochterski, J. W.; Ayala, P. Y.; Morokuma, K.; Voth, G. A.; Salvador, P.; Dannenberg, J. J.; Zakrzewski, V. G.; Dapprich, S.; Daniels, A. D.; Strain, M. C.; Farkas, O.; Malick, D. K.; Rabuck, A. D.; Raghavachari, K.; Foresman, J. B.; Ortiz, J. V.; Cui, Q.; Baboul, A. G.; Clifford, S.; Cioslowski, J.; Stefanov, B. B.; Liu, G.; Liashenko, A.; Piskorz, P.; Komaromi, I.; Martin, R. L.; Fox, D. J.; Keith, T.; Al-Laham, M. A.; Peng, C. Y.; Nanayakkara, A.; Challacombe, M.; Gill, P. M. W.; Johnson, B.; Chen, W.; Wong, M. W.; Gonzalez, C.; Pople, J. A. *Gaussian 03*, revision D.01; Gaussian, Inc.: Wallingford, CT, 2004.

(7) The different behaviour is a consequence of the fact that compound **2** is more hindered than **1**, having two methyl groups in the *ortho* positions of the aryl substituent.

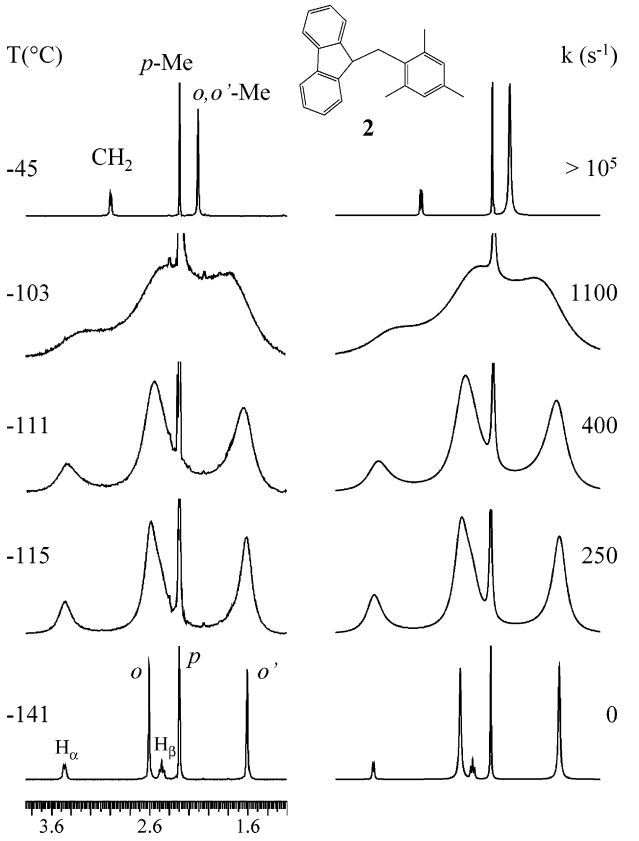

FIGURE 2. Temperature dependence of the ^{1}H (600 MHz in CHF_2-Cl/$CHFCl_2$) spectral region from 3.9 to 1.2 ppm of **2** (left). On the right the simulation obtained with the rate constants reported.

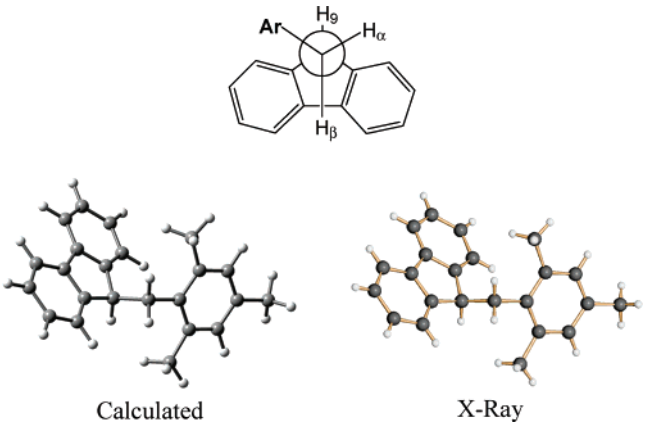

FIGURE 3. DFT computed (left) and X-ray structure (right) of compound **2** (bottom). On the top is displayed the corresponding Newman projection, where Ar is the mesityl moiety.

DFT computations predict that in the case of **2** the conformer of type B (*syn*) of Scheme 1 does not correspond to an energy minimum (actually corresponds to a transition state, as will be subsequently discussed) and the only populated ground state is that where the fluorenyl and the mesityl moieties are in an *anti* relationship (analogous to the form A of Scheme 1). The results of the calculations are confirmed by the X-ray diffraction that shows how the experimental structure is essentially equal to the computed one (Figure 3). In the corresponding Newman projection the mesityl (Ar) appears in a gauche relationship with respect to the H9 hydrogen of fluorene, thus indicating that **2** adopts an asymmetric, thus chiral, conformation (C_1 point group). This accounts for the anisochronous signals (labeled H_α and H_β) observed for the two methylene hydrogens in the −141 °C trace of the NMR spectrum in Figure 2. In this spectrum the downfield signal at 3.45 ppm (labeled H_α) appears as a doublet since there is a large J coupling with only one geminal hydrogen H_β, whereas the upfield signal at 2.46 ppm (labeled H_β) appears as a triplet, because there is an additional large coupling with the anti H_9 proton. This allowed us to assign[8] the two methylene hydrogens as shown in the Newman projection at the top of Figure 3. Such an assignment is further confirmed by the computed[6] chemical shifts that predict the H_α signal to be downfield with respect to H_β (3.68 and 2.62 ppm, respectively): the separation of the computed chemical shifts (1.06 ppm) is in even better agreement with the experiment (0.99 ppm), the deviation being only 0.07 ppm.

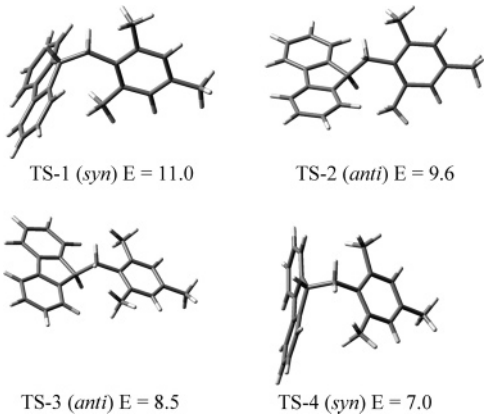

FIGURE 4. DFT computed transition states for the four possible motions that might occur in compound **2**. The energy values (in kcal mol^{-1}) are relative to the ground state of Figure 3.

The existence of a single barrier for the rotation about two different bonds suggests that these motions are probably correlated. Four possible pathways, each with its own transition state, should be in principle considered in order to explain the exchange of the diastereotopic *ortho* methyl groups and of the diastereotopic methylene hydrogens. All these pathways appear to be correlated since the visual observation of the vibrational modes, associated with the negative frequency of the transition states, shows that both the aryl−CH_2 and fluorenyl−CH_2 bonds are simultaneously involved. The corresponding computed transitions states are reported in Figure 4.

(n° I) A possible pathway is that corresponding to the correlated rotation about the mesityl−CH_2 and the fluorenyl−CH_2 bonds,[9] where the transition state (TS-1 of Figure 4) has the fluorenyl and mesityl moieties in a *syn* relationship, with one of the two *ortho* methyl groups eclipsing the C9−H9 bond

(8) At −141 °C the H9 signal of the fluorenyl moiety (4.20 ppm) is sufficiently sharp as to display a double doublet, with J values equal to 4.5 and to 11 Hz. The larger of these values, according to the Karplus relationship (see Karplus, M. *J. Am. Chem. Soc.* **1963**, 85, 2870−2871), is due to the coupling with H_β, which is in an *anti* relationship to H9 (i.e., H_9−C−C−H_β dihedral angle ≈ 180°), whilst the smaller coupling is that with H_α (i.e., H_9−C−C−H_α dihedral angle ≈ 60°). The signal of H_α thus comprises the $J \approx 4.5$ Hz and also the geminal coupling with H_β ($J \approx -15$ Hz). Owing to the quite broad line width of the methylene signals below −140 °C, however, a doublet signal is observed, because only the effect of major coupling is detectable. The signal of H_β comprises the $J \approx 11$ Hz and also the geminal coupling with H_α ($J \approx -15$ Hz). The combination of these two large couplings yields, in practice, a triplet signal since the difference between these two values cannot be detected, owing to the quite broad line width of the methylene signals below −140 °C.

of fluorene (i.e., dihedral angle C9−CH_2−C_{ipso}−C_{ortho} = 0°). This enantiomerization process has a computed barrier of 11.0 kcal mol^{-1}.

(n° II) Another possible pathway[9] is that where the transition state (TS-2 of Figure 4) has the fluorenyl and mesityl moieties in an *anti* relationship, with one of the two *ortho* methyl groups eclipsing the C9−H9 bond of fluorene (i.e., dihedral angle C9−CH_2−C_{ipso}−C_{ortho} = 0°). This enantiomerization process has a computed barrier of 9.6 kcal mol^{-1}.

(n° III) The correlated motions can also occur according to a pathway[9] where the transition state (TS-3 of Figure 4) has the fluorenyl and mesityl moieties in an *anti* relationship, with the C9−H9 bond of fluorenyl orthogonal to the mesityl ring (i.e., dihedral angle C9−CH_2−C_{ipso}−C_{ortho} = 90°) and with H9 pointing toward the mesityl moiety. This enantiomerization process has a computed barrier of 8.5 kcal mol^{-1}.

(n° IV) The last possible pathway corresponds to a process[9] where the transition state (TS-4 of Figure 4) has the fluorenyl and mesityl moieties in a *syn* relationship, with the C9−H9 bond also orthogonal to the mesityl ring (i.e., dihedral angle C9−CH_2−C_{ipso}−C_{ortho} = 90°), but with H9 pointing away from the mesityl moiety. The enantiomerization barrier computed for this pathway has the lowest value (7.0 kcal mol^{-1}, as in Table 1).

When any of these four pathways is rapid, a dynamic symmetry is created (this will make the CH_2 hydrogens enantiotopic); as a consequence they must all be frozen in order to account for the asymmetric chiral conformation corresponding to the −141 °C NMR spectrum of Figure 2. The barrier experimentally measured should be therefore the one corresponding to the fastest rate, i.e., pathway n° IV which has the transition state (TS-4 of Figure 4) with the lowest energy. This is further confirmed by the observation that the experimental barrier (7.4 kcal mol^{-1}) has a value which is very close to the lowest (7.0 kcal mol^{-1}) of the four computed barriers.

The variable temperature spectrum of compound **3** shows how the ^{1}H methyl signal of the *ortho* isopropyl groups broadens and splits into two equally intense signals below −35 °C, whereas the methyl signal of the *para* isopropyl group does not[10] (Figure 5). The experimental barrier (11.7 kcal mol^{-1}) determined from the rate constants (k_1) employed for the simulation should correspond to the transition state TS-2, i.e., the transition state involved in the faster of the two pathways (indicated as n° I and II in the case of **2**) that can make isochronous the signals of the diastereotopic methyl groups. Contrary to the case of **2** this pathway is NMR visible in **3** because the prochiral methyls of the *ortho* isopropyl groups become diastereotopic[11] when the pathway n° II (homomerisation) is frozen. Owing to the larger steric hindrance of the isopropyl with respect to the methyl groups, the computed barrier for this process is expected to be higher in **3** with respect to **2**. Indeed the computed energy value (11.7 kcal mol^{-1}) for the corresponding transition state (see TS-2 in Figure S-3 of the Supporting Information) not only is higher than that for the analogous situation of **2** but also is coincident with the experimental value, thus making quite reliable the assignment of the pathway n° II as the route responsible for the observed dynamic process reported in Figure 5 for compound **3**.

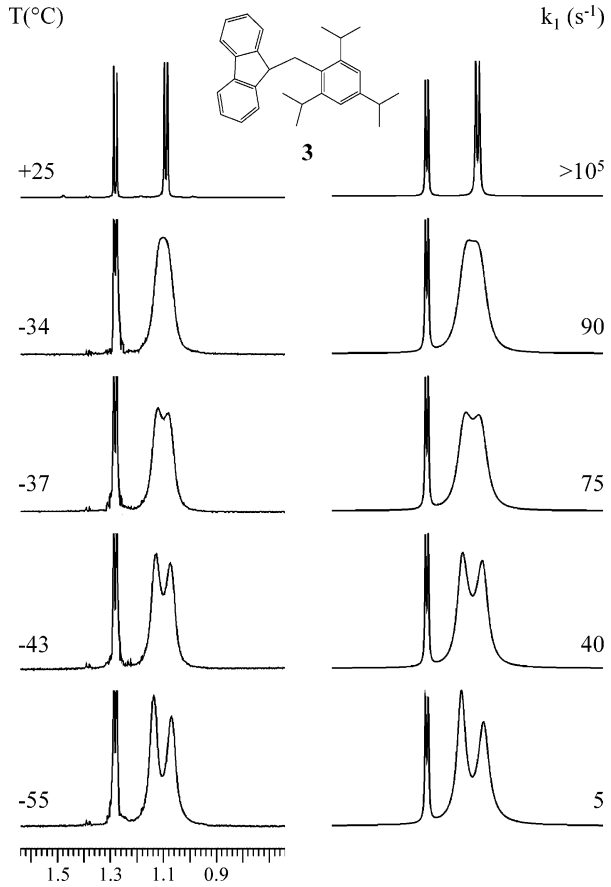

FIGURE 5. Temperature dependence (left) of the ^{1}H methyl signals of compound **3** (600 MHz in $CHF_2Cl/CHFCl_2$). The simulation, obtained with the rate constants k_1, is shown on the right.

On further lowering the temperature below −55 °C, a second process begins to take place, which was better monitored by looking to the ^{13}C spectrum of the CH carbons of the *ortho* isopropyl groups (Figure 6). From the rate constants k_2, a barrier of 7.9 kcal mol^{-1} is obtained (Table 1).

This second barrier must be related to the lowest of the four transition states having C_s symmetry. In the case of **3**, this pathway corresponds to the same type of process indicated as n° IV in the case of **2**. The computed energy of the corresponding transition state (7.4 kcal mol^{-1}, as in TS-4 of Figure S-3 of the Supporting Information) matches satisfactorily the experimental barrier of 7.9 kcal mol^{-1}.

In the ^{1}H spectrum of **4** the signals of H9, CH_2, and CH_3 remain essentially unchanged down to −130 °C but broaden

(9) These processes bear some analogy with those indicated as ring-flip pathways by Mislow et al. See: Gust, D.; Mislow, K. *J. Am. Chem. Soc.* **1972**, *95*, 1535−1547. Mislow, K. *Acc. Chem. Res.* **1976**, *9*, 26−33. Iwamura, H.; Mislow, K. *Acc. Chem. Res*. **1988**, *21*, 175−182. Mislow, K. *Chemtracts: Org. Chem.* **1989**, *2*, 151. Glaser, R. In *Acyclic Organonitrogen Stereodynamics*; Lambert, J. B., Takeuchi, Y., Eds; VCH: New York, 1992; Chapter 4. Rappoport, Z.; Biali, S. E. *Acc. Chem. Res*. **1997**, *30*, 307−314. Lindner, A. B.; Grynszpan, F.; Biali, S. E. *J. Org. Chem*. **1993**, *58*, 6662−6670. Grilli, S.; Lunazzi, L.; Mazzanti, A.; Casarini, D.; Femoni, C. *J. Org. Chem.* **2001**, *66*, 488−495. Grilli, S.; Lunazzi, L.; Mazzanti, A.; Mazzanti, G. *J. Org. Chem.* **2001**, *66*, 748−754. Grilli, S.; Lunazzi, L.; Mazzanti, A. *J. Org. Chem.* **2001**, *66*, 4444−4446. Grilli, S.; Lunazzi, L.; Mazzanti, A. *J. Org. Chem.* **2001**, *66*, 5853−5858.

(10) The doublet due to the coupling with the isopropyl CH hydrogen is not visible anymore at low temperature in the case of the methyl signal of the *ortho* isopropyl groups because the corresponding line width is broadened by a second motion (see Figure 6) which begins to affect the spectrum. This broadening does not occur for the methyl signal of the *para* isopropyl group because the latter is not affected by the mentioned second motion.

(11) Mislow, K.; Raban, M. *Top. Stereochem.* **1967**, *1*, 1. Jennings, W. B. *Chem. Rev.* **1975**, *75*, 307. Eliel, E. L. *J. Chem. Educ*. **1980**, *57*, 52. Casarini, D.; Lunazzi, L.; Macciantelli, D. *J. Chem. Soc., Perkin Trans 2* **1992**, 1363.

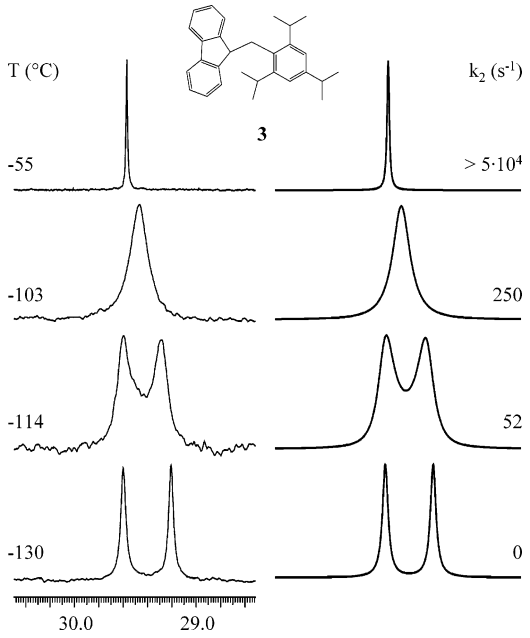

FIGURE 6. Temperature dependence (left) of the ^{13}C NMR CH signal of the *ortho* isopropyl groups (150.8 MHz in $CHF_2Cl/CHFCl_2$) of compound **3**. On the right is shown the simulation obtained with the rate constants (k_2) employed.

considerably on further cooling and eventually split, at −173 °C, into two (H9 and CH_3) and three (CH_2) signals, with a 70:30 intensity ratio (Figure 7). This proves that two conformers have been detected, as a consequence of the restricted rotation about the tolyl−CH_2 and fluorenyl−CH_2 bonds. The barrier for interconverting the more into the less populated conformer is 5.3 kcal mol^{-1}, as determined by the line shape simulation (Figure S-4 of the Supporting Information). The spectrum of the major conformer displays two anisochronous lines (labeled H_α and H_β in Figure 7) due to the diastereotopicity of the methylene hydrogens (the line width is too broad at this low temperature to display the splitting due to the geminal coupling), whereas a single line is observed for the CH_2 hydrogens of the minor form.

DFT computations predict indeed the existence of two energy minima, corresponding to two ground states, separated by an energy difference of 0.13 kcal mol^{-1}, both having the aryl and fluorenyl moieties in an *anti* relationship. As shown in Scheme 2 one conformer (labeled C) has the Me group pointing toward H9 of the fluorene ring, whereas the other (labeled D) points away from it. The interconversion of the conformers C and D can take place *via* a correlated rotation about the tolyl−CH_2 and fluorenyl−CH_2 bonds. In the corresponding transition state, the tolyl ring is othogonal to the C9−CH_2 bond (i.e., dihedral angle C9−CH_2−C_{ipso}−C_{ortho} ≈ 90°), with a DFT computed energy (4.7 kcal mol^{-1}) which is in fair agreement with the barrier (5.3 kcal mol^{-1}, as in Table 1) measured for the conformer interconversion (see Figure S-5 of the Supporting Information). This process thus corresponds to the pathway of type n° III mentioned above.

To the more populated conformer the enantiomeric structures C and C′ of Scheme 2 should be assigned, because here the two CH_2 hydrogens (α and β) must be diastereotopic, thus accounting for the observed anisochronous lines at −173 °C (Figure 7). The less populated conformer must have the structure D, since in this conformer the small amplitude torsion process,

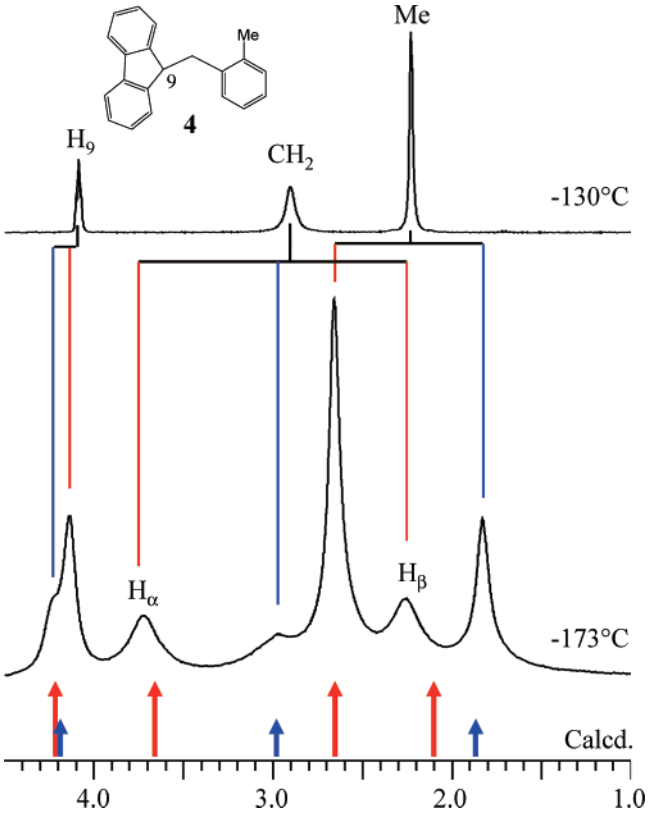

FIGURE 7. ^1H NMR spectrum (600 MHz in $CHF_2Cl/CHFCl_2$) of the aliphatic region of **4** at two different temperatures. The arrows (red for the major and blue for the minor conformer) represent the DFT calculated shifts (all moved upfield by 0.16 ppm).

SCHEME 2. Schematic Representations of the Equilibrium between the Enantiomers of the Two Most Stable Conformers and X-ray Structure of Compound 4

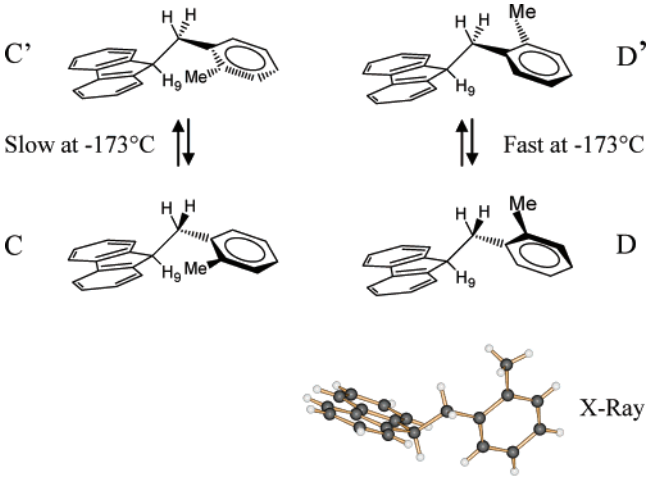

interconverting D with its enantiomer D′, has a transition state where the methyl crosses over the CH_2 hydrogens (dihedral angle C9−CH_2−C_{ipso}−C_{ortho} ≈ 180°). According to DFT computations this torsion process is expected to be very fast, having a predicted barrier of only 3.9 kcal mol^{-1}, which is a value too small to be detected in an NMR experiment (See Figure S-5 of the Supporting Information). This fast motion generates a dynamic plane of symmetry (a situation similar to that occurring in conformer A of compound **1** reported in

Scheme 1), which makes the methylene hydrogens α and *β* of the minor conformer equivalent (enantiotopic), as experimentally observed.

The computed ground state energy for conformer D is 0.13 kcal mol^{-1} lower than that of C, in apparent contradiction with the assignment above. When such small energy differences are involved, the approximations of the calculations make the results not very reliable. In these cases a more satisfactory approach is that based on the computed values of chemical shifts, if the latter are significantly different. DFT calculations indicate that the upfield methyl signal, which is the less intense in the experimental spectrum (Figure 7), is that of conformer D,[12] confirming that the latter should be the less populated one. Also, the computed separation for the signals of the diastereotopic methylene hydrogens (H_α and H_β) of conformer C is 1.55 ppm, in agreement with the 1.47 ppm separation observed for the corresponding signals of the major conformer (Figure 7). In addition, the average value of the computed methylene shifts of conformer D lies in between the two signals of conformer C.[13] Since in the experimental spectrum (Figure 7) the intensity of the single CH_2 signal is lower than that of the pair of anisochronous CH_2 signals, the assignment of C as the more stable, and D as the less stable, conformer in solution is further supported.

The structure of compound **4**, obtained by single-crystal X-ray diffraction, resembles quite closely (Scheme 2) that of the less populated conformer D. It is not unusual to encounter differences between the conformations in solids and in solution, which depend on the fact that crystals privilege the conformation which fits better the crystal cell.[14,15] This feature further indicates that the energies of the two conformers are quite similar and that their relative populations are strongly dependent on the environment.[16]

Analogous results, as should be expected, were obtained in the case of the similar compound **5**, which has an isopropyl replacing the *ortho* methyl group. The ^{1}H NMR of the signal of the aliphatic hydrogens (with the exception of that of H9) split, at −162 °C, into two groups of lines, with a 70:30 intensity ratio (Figure 8). Again the methylene of the major conformer yields two anisochronous lines, due to the diastereotopicity of the corresponding hydrogens (the line width is too broad at this low temperature to display the splitting due to the geminal coupling). On the contrary, the methylene hydrogens of the minor conformer display a single line. Thus to the major form should be assigned the asymmetric structure (C_1 point group) of the same type C displayed in Scheme 2 for **4**, and to the minor that of type D, where the fast torsion process makes the methylene signals equivalent (isochronous) owing to the mentioned C_s dynamic symmetry. This assignment is further confirmed by the trend of the DFT computed chemical shifts reported in Figure 8.[17]

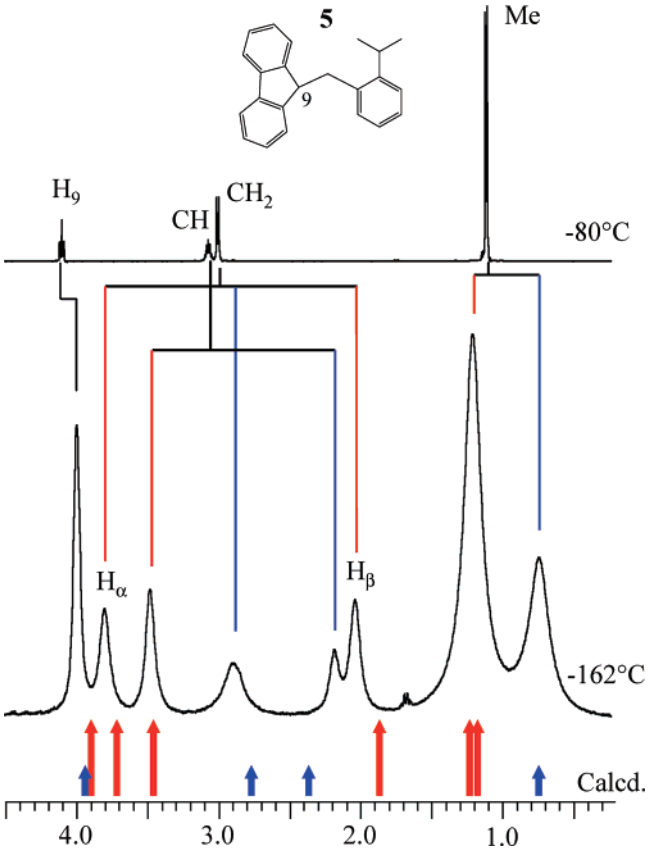

FIGURE 8. ^{1}H NMR spectrum (600 MHz in $CHF_2Cl/CHFCl_2$) of the aliphatic region of **5** at two different temperatures. The arrows (red for the major and blue for the minor conformer) represent the DFT calculated shifts (all moved upfield by 0.34 ppm).

The line shape simulation (Figure S-6 of the Supporting Information) of the aliphatic signals yields a barrier for the interconversion equal to 5.6 kcal mol^{-1}. As in the case of **4** this process can be attributed to the correlated motion of type n° III, since the corresponding computed transition state (analgous to TS-3 of Figure 4 and of Figure S-3 of the Supporting Information) has an energy of 4.65 kcal mol^{-1} (Table 1), quite close to the experimental value. In the present case it has been also possible to observe experimentally a further consequence of the restricted rotations involving both the aryl−CH_2 and the fluorenyl−CH_2 bonds. As expected on the basis of the correlated rotation processes, in fact, the ^{13}C spectrum of **5** at −162 °C shows that the major conformer displays two anisochronous signals (Figure S-7 of the Supporting Information) for the quaternary carbons in positions 10 and 11 of the

(12) The computed difference between the methyl shifts of conformers C and D is 0.77 ppm, which agrees well with the experimental separation of 0.83 ppm.

(13) The two CH_2 shifts of conformer D (3.70 and 2.58 ppm) must be averaged, owing to the mentioned fast torsion process which creates the dynamic C_s symmetry for this conformer. Computations predict that this averaged shift lies in between the pair of CH_2 signals of C and that the upfield signal of the latter is separated by that of D by 0.79 ppm, in fair agreement with the 0.69 ppm separation experimentally observed (Figure 7).

(14) Johansen, J. T.; Vallee, B. L. *Proc. Natl. Acad. Sci. U.S.A.* **1971**, *68*, 2532−2535. Kessler, H. *Fresenius Z. Anal. Chem.* **1987**, *327*, 66−67. Burke, L. P.; DeBellis, A. D.; Fuhrer, H.; Meier, H.; Pastor, S. D.; Rihs, G.; Rist, G.; Rodebaugh, R. K.; Shum, S. P. *J. Am. Chem. Soc.* **1997**, *119*, 8313−8323. Paulus, E. F.; Kurz, M.; Matter, H.; Vértesy, L. *J. Am. Chem. Soc.* **1998**, *120*, 8209−8221. Perry, N. B.; Blunt, J. W.; Munro, M. H. *Magn. Reson. Chem.* **2005**, *27*, 624−627.

(15) A situation where it has been unambiguously demonstrated that the X-ray diffraction structure in the solids is that of the minor conformer present in solution has been reported in: Lunazzi, L.; Mazzanti, A.; Minzoni, M.; Anderson, J. E. *Org. Lett.* **2005**, **7**, 1291−1294.

(16) A recent example where the type of conformer observed in the crystal depends on the crystallisation solvent was reported in: Coluccini, C.; Grilli, S.; Lunazzi, L.; Mazzanti, A. *J. Org. Chem.* **2003**, *68*, 7266−7273.

(17) The isopropyl methyl signals of **5** should be anisochronous in the −162 °C spectrum of the major conformer, but the corresponding shift difference is smaller than the line width (about 85 Hz at this temperature). This is confirmed by the computed shift separation, which is predicted to be only 0.04 ppm (i.e., 24 Hz at 600 MHz).

SCHEME 3. Reaction Scheme for the Preparation of 1−5

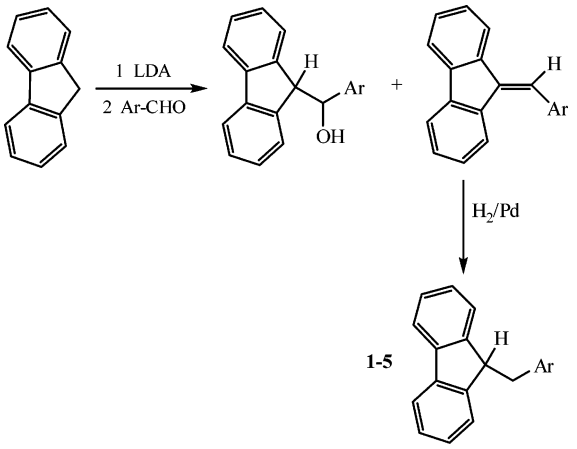

fluorenyl moiety (the minor conformer still displays a single line for this pair of carbons, due to the dynamic C_s symmetry generated by the small amplitude torsion previously discussed).

Summary. The stereodynamic processes occurring in fluorenes derivatives, having a number of substituted benzyl groups bonded to position 9, were monitored by variable temperature NMR spectroscopy. Depending on the type of benzyl substituents, conformers of different stabilities (like in **1**, **4**, **5**) and enantiomeric forms (like in **2**, **3**) were observed at very low temperatures. The structures of two such conformers (compound **2** and **4**) were also determined by single-crystal X-ray diffraction and were found to agree with the predictions of DFT calculations. The interconversion processes were interpreted as being due to correlated rotation pathways, as suggested by DFT calculations that indicated the appropriate transition states reproducing the experimental barriers in a satisfactory manner.

Experimental Section

Materials: 2-Methyl-benzaldehyde and 2,4,6-trimethylbenzaldehyde were commercially available. **1-Bromo-3,5-diisopropylbenzene** was prepared according to the literature.[18]

2-Isopropylbenzaldehyde, **3,5-diisopropylbenzaldehyde**, and **2,4,6-triisopropylbenzaldehyde**[19] were prepared following known procedures (see the Supporting Information for details). Compounds **1**−**5** were achieved by reacting 9-fluorene with the requested aromatic aldehydes and reducing the intermediate alkenes, as reported in Scheme 3.

General Procedure for 1−5: To a stirred solution of *N*,*N*-diisopropylamine (1.1 mL, 8 mmol in 30 mL of anhydrous THF) kept at −10 °C under nitrogen, 5.5 mL (8.5 mmol, 1.6 M solution) of *n*-BuLi were slowly added. The mixture was allowed to react at −10 °C for 30 min and then slowly transferred by a double-tipped needle into a solution of 9-fluorene (1.0 g, 6 mmol in 25 mL of anhydrous THF) kept at −15 °C. The resulting yellow solution was stirred at −15 °C for additional 20 min, and then a solution of the appropriate aldehyde (10 mmol in 10 mL of dry THF) was added in 10 min. The yellow solution faded during addition, and after stirring for 15 min the reaction was quenched with 20 mL of H_2O. The extracted organic layer (Et_2O) was dried (Na_2SO_4) and evaporated. The crude, a mixture of alkene and alcohol, was purified by a silica gel chromatography column (petroleum ether/EtAc 95:5 v/v) to give the intermediate alkenes (yield 62−70%). Spectroscopic data of the alkenes are reported in the Supporting Information.

In a 150 mL reaction bottle of the Parr apparatus was fitted a solution of the appropriate alkene (about 4 mmol in 10 mL of THF and 60 mL of MeOH), and then 100 mg of catalyst Pd/C 5% were added and the suspension was shaken under H_2 pressure ($\approx$ 2 bar) at room temperature. After 2 h the reaction was completed. The catalyst was filtered off. and the solvent evaporated to give the desired benzylfluorenes **1**−**5** almost in a quantitative yield.

Analytically pure samples were obtained by semipreparative HPLC using C18 or C8 columns (5 μm, 250 mm × 10 mm, 5 mL/min, ACN/H_2O 70:30 v/v or 80:20 v/v). Crystals suitable for X-ray diffraction were obtained for **2** and **4** by slow evaporation of the solvent (hexane in both cases).

9-(3,5-Diisopropylbenzyl)-9*H*-fluorene (1). ^{1}H NMR (600 MHz, $CDCl_3$, 25 °C, TMS): δ 1.23 (12H, d, J = 6.9 Hz), 2.86 (2H, m, J = 6.9 Hz), 3.09 (2H, d, J = 7.9 Hz), 4.22 (1H, t, J = 7.9 Hz), 6.88 (2H, d, J = 1.6 Hz), 6.95 (1H, br t, J = 1.6 Hz), 7.19 (2H, d, J = 7.5 Hz), 7.22 (2H, dt, J = 7.5, 1.0 Hz),7.34 (2H, t, J = 7.1 Hz), 7.73 (2H, d, J = 7.7 Hz). ^{13}C NMR (150.8 MHz, $CDCl_3$, 25 °C, TMS) δ 24.1 ($4CH_3$), 34.1 (2CH), 40.3 (CH_2), 48.9 (CH), 119.7 (2CH), 122.8 (CH), 125.0 (2CH), 125.1 (2CH), 126.5 (2CH), 127.0 (2CH), 139.3 (Cq), 140.8 (2Cq), 146.9 (2Cq), 148.7 (2Cq). HRMS-(EI): *m*/*z* calcd for $C_{26}H_{28}$, 340.21910; found, 340.2192.

9-(2,4,6-Trimethylbenzyl)-9*H*-fluorene (2). Mp 94−96 °C. ^{1}H NMR (600 MHz, $CDCl_3$, 25 °C, TMS): δ 2.19 (6H, s), 2.37 (3H, s), 3.07 (2H, d, J = 8.7 Hz), 4.22 (1H, t, J = 8.7 Hz), 6.94 (2H, s), 7.09 (2H, d, J = 7.7 Hz), 7.22 (2H, dt, J = 7.4, 1.1 Hz), 7.38 (2H, t, J = 7.5 Hz), 7.80 (2H, d, J = 7.6 Hz). ^{13}C NMR (150.8 MHz, $CDCl_3$, 25 °C, TMS): δ 20.3 ($2CH_3$), 20.9 (CH_3), 33.8 (CH_2), 46.2 (CH), 119.8 (2CH), 124.8 (2CH), 126.6 (2CH), 127.0 (2CH), 129.1 (2CH), 133.6 (Cq), 135.6 (Cq), 137.0 (2Cq), 140.7 (2Cq), 147.1 (2Cq). HRMS(EI): *m*/*z* calcd for $C_{23}H_{22}$, 298.17215; found, 298.1721.

9-(2,4,6-Triisopropylbenzyl)-9*H*-fluorene (3). ^{1}H NMR (600 MHz, $CDCl_3$, 25 °C, TMS): δ 1.13 (12H, d, J = 6.9 Hz), 1.32 (6H, d, J = 6.9 Hz), 2.94 (1H, m, J = 6.9 Hz), 3.01 (2H, m, J = 6.9 Hz), 3.14 (2H, d, J = 8.8 Hz), 4.13 (1H, t, J = 8.8 Hz), 7.02 (2H, d, J = 7.6 Hz), 7.05 (2H, s), 7.19 (2H, dt, J = 7.5, 0.9 Hz), 7.35 (2H, t, J = 7.5 Hz), 7.78 (2H, d, J = 7.5 Hz). ^{13}C NMR (150.8 MHz, $CDCl_3$, 25 °C, TMS): δ 24.1 ($4CH_3$, broad), 24.2 ($2CH_3$), 29.5 (2CH), 31.4 (CH_2), 34.2 (CH), 48.1 (CH), 119.8 (2CH), 120.8 (2CH), 125.0 (2CH), 126.5 (2CH), 127.0 (2CH), 130.7 (Cq), 140.6 (2Cq), 146.9 (2Cq), 147.1 (Cq), 147.4 (2Cq). HRMS-(EI): *m*/*z* calcd for $C_{29}H_{34}$, 382.26605; found, 382.2662.

9-(2-Methylbenzyl)-9*H*-fluorene (4).[20] Mp 72−73 °C. ^{1}H NMR (600 MHz, $CDCl_3$, 25 °C, TMS): δ 2.26 (3H, s), 3.04 (2H, d, J = 8.3 Hz), 4.19 (1H, t, J = 8.3 Hz), 7.10 (2H, d, J = 7.6 Hz), 7.19 (2H, t, J = 8.2 Hz), 7.22 (3H, br s), 7.26 (1H, br m), 7.35 (2H, t, J = 7.4 Hz), 7.75(2H, d, J = 7.6 Hz). ^{13}C NMR (150.8 MHz, $CDCl_3$, 25 °C, TMS): δ 19.7 (CH_3), 37.7 (CH_2), 47.6 (CH), 119.8 (2CH), 124.8 (2CH), 125.9 (CH), 126.6 (CH), 126.7 (2CH), 127.1 (2CH), 130.4 (CH), 130.4 (CH), 136.7 (Cq), 138.4 (Cq), 140.7 (2Cq), 147.0 (2Cq). HRMS(EI): *m*/*z* calcd for $C_{21}H_{18}$, 270.14085; found, 270.1409.

9-(2-Isopropylbenzyl)-9*H*-fluorene (5). Mp 88−89 °C. ^{1}H NMR (600 MHz, $CDCl_3$, 25 °C, TMS): δ 1.20 (6H, d, J = 6.9 Hz), 3.11 (2H, d, J = 8.3 Hz), 3.15 (1H, m, J = 6.9 Hz), 4.20 (1H, t, J = 8.3 Hz), 7.09 (2H, d, J = 7.5 Hz), 7.22 (3H, dt, J = 6.9, 1.0 Hz), 7.26(1H, m), 8.0 (1H, m), 7.33 (1H, dt, J = 7.4, 1.5 Hz), 7.37 (3H, t, J = 7.4 Hz), 7.79 (2H, d, J = 7.9 Hz). ^{13}C NMR (150.8 MHz, $CDCl_3$, 25 °C, TMS): δ 23.9 ($2CH_3$), 28.8 (CH), 37.0 (CH_2), 48.6 (CH), 119.8 (2CH), 124.9 (2CH), 125,4 (CH), 125.5 (CH), 126.6 (2CH), 127.0 (2CH), 127.1 (CH), 130.8 (CH), 136.8 (Cq), 140.7 (Cq), 146.9 (2Cq), 147.3 (Cq). HRMS(EI): *m*/*z* calcd for $C_{23}H_{22}$, 298.17215; found, 298.1722.

(18) Diemer, V.; Chaumeil, H.; Defoin, A.; Fort, A.; Boeglin, A.; Carré, C. *Eur. J. Org. Chem.* **2006**, 2727−2738. Liu, R; Gomes, P. T.; Costa, S. I.; Duarte, M. T.; Braquinho, R.; Fernandes, A. C.; Chien, J. C. W.; Singh, R. P.; Marques, M. M. *J. Organomet. Chem.* **2005**, *690*, 1314−1323.

(19) Casarini, D.; Lunazzi, L.; Verbeeck, R. *Tetrahedron* **1996**, *52*, 2471−2480. Rieche, A.; Gross, H.; Höft, E. *Org. Synth.* **1967**, *47*, 51.

(20) Sieglitz, A.; Jassoy, H. *Ber. D. Chem.* **1921**, *54B*, 2133−2138.

NMR Spectroscopy. The spectra were recorded at 600 MHz for ^{1}H and 150.8 MHz for ^{13}C. The assignments of the ^{1}H and ^{13}C signals were obtained by bidimensional experiments (edited-gHSQC[21] and gHMBC[22] sequences). The samples for obtaining spectra at temperatures lower than −100 °C were prepared by connecting to a vacuum line the NMR tubes containing the compound and a small amount of C_6D_6 (for locking purpose) and condensing therein the gaseous CHF_2Cl and $CHFCl_2$ (4:1 v/v) under cooling with liquid nitrogen. The tubes were subsequently sealed in *vacuo* and introduced into the precooled probe of the spectrometer. Low temperature ^{13}C spectra were acquired with a 5 mm dual probe, without spinning, with a sweep width of 38 000 Hz, a pulse width of 4.9 μs (70° tip angle), and a delay time of 2.0 s. Proton decoupling was achieved with the standard Waltz-16 sequence. A line broadening function of 1−5 Hz was applied to the FIDs before Fourier transformation. Usually 512 to 1024 scans were acquired. Temperature calibrations were performed before the experiments, using a Cu/Ni thermocouple immersed in a dummy sample tube filled with isopentane and under conditions as nearly identical as possible. The uncertainty in the temperatures was estimated from the calibration curve to be ±2 °C. The line shape simulations were performed by means of a PC version of the QCPE program DNMR 6 n° 633, Indiana University, Bloomington, IN.

Calculations. Geometry optimization were carried out at the B3LYP/6-31G(d) level by means of the Gaussian 03 series of programs[6] (see the Supporting Information): the standard Berny algorithm in redundant internal coordinates and default criteria of convergence were employed. The reported energy values are not ZPE corrected. Harmonic vibrational frequencies were calculated for all the stationary points. For each optimized ground state the frequency analysis showed the absence of imaginary frequencies, whereas each transition state showed a single imaginary frequency. Visual inspection of the corresponding normal mode was used to confirm that the correct transition state had been found. NMR chemical shift calculations were obtained with the GIAO method at the B3LYP/6-311+G(d,p)//B3LYP/6-31G(d) level. TMS, calculated at the same level of theory, was used as a reference to scale the absolute shielding value.

Acknowledgment. L.L. and A.M. received financial support from the University of Bologna (RFO) and from MUR-COFIN 2005, Rome (national project "Stereoselection in Organic Synthesis").

Supporting Information Available: DFT computed structures of the two most stable conformers (A and B) of compound **1**; DFT computed transition states of **3**; Computed energy diagram for compound **4**; variable temperature NMR spectra of compounds **2**, **4**, and **5**; experimental details and spectroscopic data for the reaction intermediates; X-ray data of compounds **2** and **4**; ^{1}H, ^{13}C NMR spectra and HPLC traces of **1**−**5**; chemical shift calculations of **2**, **4**, and **5**; computational data of **1**−**6**. This material is available free of charge via the Internet at http://pubs.acs.org.

JO7026917

(21) Bradley, S. A.; Krishnamurthy, K. *Magn. Res. Chem.* **2005**, *43*, 117−123. Willker, W.; Leibfritz, D.; Kerssebaum, R.; Bermel, W. *Magn. Res. Chem.* **1993**, *31*, 287−292.

(22) Hurd, R. E.; John, B. K. *J. Magn. Reson.* **1991**, *91*, 648−653.